

INVERSION TECHNIQUES IN THE SOFT-X-RAY TOMOGRAPHY OF FUSION PLASMAS: TOWARD REAL-TIME APPLICATIONS

J. MLYNAR,^{a*} V. WEINZETTL,^a G. BONHEURE,^b A. MURARI,^c and JET-EFDA CONTRIBUTORS[†]

JET-EFDA, Culham Science Centre, OX14 3DB, Abingdon, United Kingdom

^a*Association EURATOM/IPP.CR, Institute of Plasma Physics AS CR, v.v.i., Za Slovankou 3, CZ-18200 Praha 8 Czech Republic*

^b*Association EURATOM/Etat Belge, ERM-KMS, B1000 Brussels, Belgium*

^c*Association EURATOM/ENEA, Consorzio RFX, I-35127 Padova, Italy*

Received March 15, 2010

Accepted for Publication May 13, 2010

The tomography of fusion plasmas provides local information on plasma emissivity from line-integrated measurements (projections). However, the corresponding inversion task presents an ill-posed and often under-determined problem. Compared to industrial and medical tomography systems, data in fusion research are spatially sparse due to the limited number of lines of sight, and they may vary rapidly in time. Therefore, dedicated inversion techniques have been developed that allow for lower spatial resolution and implementation of a priori information and constraints. In this contribution, the main

inversion techniques used today are reviewed, with working results and challenges outlined. Special attention is given to techniques that allow for rapid tomography inversions, because of their future potential for real-time applications, and a new combined technique is proposed.

KEYWORDS: *plasma tomography, real-time control, soft-X-ray diagnostics*

Note: Some figures in this paper are in color only in the electronic version.

I. INTRODUCTION

Several diagnostic systems in magnetically confined fusion plasmas provide line-integrated measurements along chords, including bolometry, visible light, soft-X-ray (SXR), or neutron diagnostics. The task of retrieval of spatial distribution of the plasma emissivity from the line-integrated measurements constitutes an important part of fusion data analyses. Solutions in general rely on the basic symmetries of the confining magnetic field. One-dimensional distribution (profile) inversion is adequate in the case of constant emissivity on magnetic flux surfaces; however, a two-dimensional (2-D) inversion is required whenever the poloidal symmetry breaks down,

e.g., due to collective magnetohydrodynamic (MHD) phenomena, impurities, or fast trapped particle effects. The emissivity distribution can be either retrieved iteratively via forward-fitting of the line integrals from the presumed local plasma emissivity or calculated directly from the measured line integrals using inversion techniques (plasma tomography; see Ref. 1). Clearly, the latter strategy has a considerable advantage of independence on plasma models but calls for a dense coverage of the plasma cross section by good measurements. The methods and challenges of inversion techniques in tomography of fusion plasmas are detailed in Sec. II.

Tomography inversion of SXR measurements has found widespread application in fusion experiments for many reasons. To start with, it is possible to build SXR diagnostics based on relatively compact and low-cost pinhole cameras with beryllium foil shielded photodiode arrays as detectors. These cameras are typically sensitive to photon energies in the kilo-electron-volt range and

*E-mail: mlynar@ipp.cas.cz

[†]See the Appendix of F. Romanelli et al., "Overview of JET Results," *Proceedings of the 22nd IAEA Fusion Energy Conference 2008*, Geneva, Switzerland.

have a very good temporal resolution (up to 1 MHz). Note that a limited spectral resolution can be achieved by using Be foils of different thicknesses² or via impurity modeling.³ Alternatively, a proper SXR imaging spectrometer⁴ can in principle be extended into a full 2-D setup. Toroidal symmetry can be investigated by installing several tomography systems.⁵ Moreover, plasma emissivity in this photon energy range is expected to be relatively smooth, with radiation intensity depending on plasma density, temperature, and effective charge, and therefore can provide information on impurity transport, MHD activities, and importantly plasma position. Recent DIII-D results⁶ demonstrated the benefits of spatially resolved SXR data for magnetic equilibrium reconstruction and concluded that the SXR diagnostics can even be used as a simplified alternative to the motional Stark effect diagnostics in determination of the q profile. Unfortunately, the simple photodiode arrays are not relevant for diagnostics of burning plasmas⁷ because of their low radiation hardness. Alternative radiation-resistant SXR cameras are under development, based on vacuum photodiode arrays⁸ or micropattern gas detectors⁹; this research deserves attention particularly when considering potential applications of plasma tomography in real-time control of plasma operation. Real-time control implies that the software and hardware systems are subject to operational deadlines from event to system response. In fusion plasmas the deadlines depend on the process controlled and typically range from milliseconds to seconds. The potential of the real-time applications in fusion plasmas has increased significantly through ongoing progress in computing power and speed. At the same time, these applications have become vital for advanced fusion experiments because of the present requirements on the real-time control of several plasma actuators.¹⁰ Recent developments in the field of rapid SXR tomography will be reviewed in Sec. III. Discussion on inversion techniques adequate for real-time SXR tomography of noncircular fusion plasmas will conclude the paper in Sec. IV.

II. INVERSION TECHNIQUES FOR FUSION PLASMA EXPERIMENTS

Tomography inversion, in general, deals with image reconstruction from the image projections. An analytical solution, known as the inverse Radon transform,¹¹ can be found. This transform represents a typical example of an ill-posed problem. The ill-posed problems, by definition, do not fulfill Hadamard’s postulates on well posedness: the existence of a solution, its uniqueness, and its continuous dependence on the data. Therefore, in practical terms, the inverse Radon transform is quite sensitive to minor changes in the input data: Any imperfection in the projection data may result in major artifacts in the recon-

structed image. That is, for the 2-D tomography inversion of the image distribution $g(x, y)$, a complete and accurate knowledge of 2-D projection function $f(p, \vartheta)$ is required; see Fig. 1. Data in medical or industrial applications of tomography are often close to this ideal condition, so that analytical inversion on filtered data is appropriate, e.g., via the filtered backprojection (FBP) technique.¹¹

Unfortunately, FBP and other market solutions of tomography inversion are not adequate for fusion plasmas where data are sparse in the available projections, particularly because the diagnostic cameras can be installed only at a few poloidal angles. Figure 2 gives a new example¹² of a typical SXR pinhole camera system setup in a fusion plasma experiment (Fig. 2a) in coordinates x, y showing diagnostic chords in the cross section of the vacuum vessel and (Fig. 2b) in coordinates p, ϑ as introduced in Fig. 1, transforming the cross section into the so-called projection space; for other examples see Ref. 13.

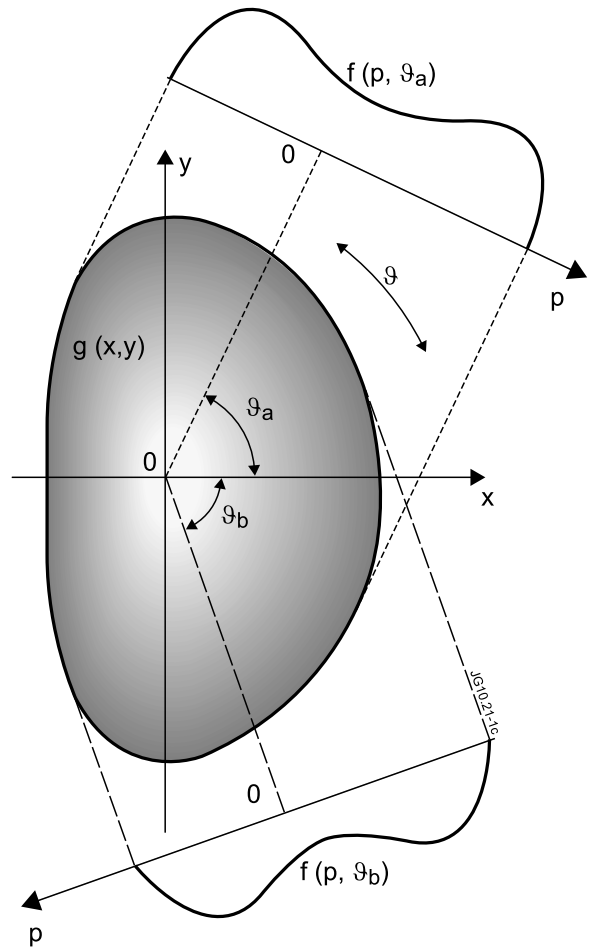


Fig. 1. Principle of 2-D tomography inversion: 2-D image distribution $g(x, y)$ is to be reconstructed from 2-D projection function $f(p, \vartheta)$ as measured by line-integrated diagnostics.

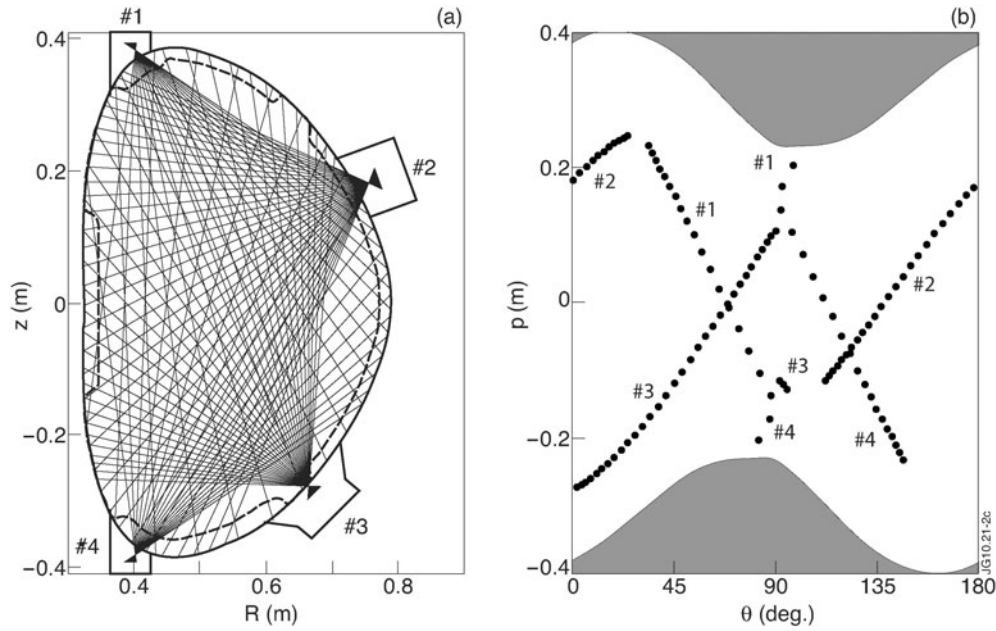


Fig. 2. Soft-X-ray tomographic system on tokamak COMPASS, under construction.¹² (a) Experimental setup of the pinhole SXR cameras in a poloidal cross section. (b) The same setup in the projection space, including the vacuum vessel shape (gray shaded). Note that lines of sight in (a) map to dots in (b).

Notice that for a proper analytical inversion, the whole white area in the projection space would have to be covered by the line-integrated measurements indicated by black dots.

In the case of sparse data, regularized algebraic techniques can be efficient, where the image is expanded into series of orthogonal basis functions $b_j(x, y)$:

$$g(x, y) = \sum_j b_j(x, y) g_j. \quad (1)$$

Note that the choice of basis function may predetermine the geometric requirements. For example, A. M. Cormack^a demonstrated that there is an unequivocal relation between expansion of the image into Zernike polynomials (in the radial coordinate) and expansion of the projections into Chebyshev functions of the second kind (in the p coordinate).¹⁴ The inversion is therefore straightforward, but because of the necessary series truncation in the polar coordinate system, the Cormack technique is not suitable for off-centered and noncircular plasmas. The Fourier-Bessel technique¹⁵ is based on the same principle but suits better the case of zero emissivity circular border and allows for considerably faster computing because of application of the Bessel functions with no singularities.

The main suite of inversion techniques for fusion plasmas takes as the starting point the linear link that

^aAlan M. Cormack (1924–1998) pioneered the applications of computed tomography in medicine (Nobel Prize 1979).

Eq. (1) implicitly establishes between the amplitudes g_j and a finite number of line-integrated measurements f_i :

$$f_i = \sum_j T_{ij} g_j, \quad (2)$$

where T_{ij} is the contribution matrix. In the most basic set of basis functions—the regular mesh of square pixels; see Fig. 3—the geometric matrix corresponds to the length of the i 'th chord in the j 'th pixel provided that the angular width of each chord is neglected. Some improvement in the tomography inversion can be achieved if the real angular width is implemented in the contribution matrix; see Ref. 1, Sec. IV.D.3. More importantly, a continuous local basis function defined on the regular mesh can be used—e.g., the bilinear interpolative functions¹³—in order to decrease the mesh density without hampering the discretization error. This allows for a smaller contribution matrix that presents a significant asset for the real-time applications. Notice that the contribution matrix is sparse, which grants some numerical advantage but implies that the task of solving Eq. (2) for unknown amplitudes g_j is indeed ill posed.

In plasma tomography, the ill-posed task of finding an inverse solution of Eq. (2) is in most cases also underdetermined; i.e., the number of base functions exceeds the number of line-integrated measurements. The regularized inversion techniques have generally few problems coping with underdetermined tasks since additional information has to be included anyway in order to find a

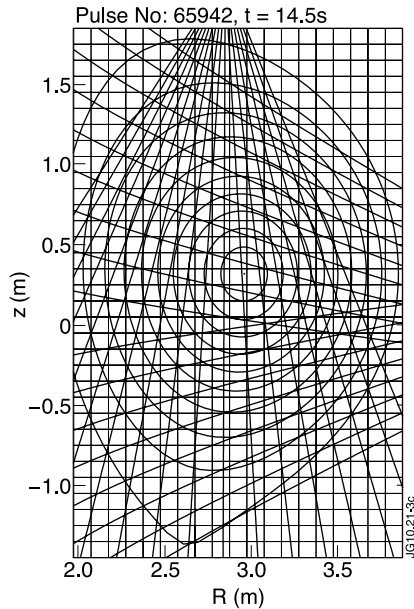


Fig. 3. Regular mesh of square pixels on the background of the SXR chords and characteristic flux surfaces at JET. Some chords are bent in this poloidal cross section because of their nonzero angle in the toroidal direction. The size of each square pixel is 10×10 cm in this mesh typical also for the JET neutron tomography.¹⁶ Figures 4 and 5 are derived in this setup.

unique solution. The additional information is introduced in the form of a priori information (inherent to the inversion technique) and in the form of constraints that set quantitative limits. The physics of the SXR plasma emission offers manifold constraints, including expected noise, nonnegativity, and zero emissivity from the border. The foremost example of a priori information is the expected smoothness of the reconstructed image. Inversion techniques solving Eq. (2) implement a priori information via the objective functional; see Ref. 1, Sec. IV.F.3. The objective functional may represent the image smoothness in the form of the second derivative operator. In an optimization algorithm, the objective functional penalizes inverse solutions that deviate from the desired property of the image. As a matter of fact, line-integrated measurements can be regarded purely as one of the optimization constraints in these inversion techniques.

A broad range of inversion techniques that find regularized solution of Eq. (2) has been developed; for an in-depth overview see Ref. 1. To sum up, an important distinguishing criterion is the choice of the objective functional (an example of a particular choice is the maximum entropy technique^{17,18}). Next, inversion techniques are categorized according to methods of selection of the regularization parameter (e.g., truncated singular value decomposition¹⁹ versus Lagrange multipliers^{13,20}). In addition, inversion techniques may be distinguished by

the optimization strategy (e.g., techniques based on Tikhonov regularization²¹ versus neural networks²²). Some inversion techniques allow for straightforward implementation of the constraints—in particular, the Lagrange multipliers—while others have very limited options in this respect. In general, categorization of the inversion techniques in the literature is not definite, and in reality some of them differ only slightly, e.g., the Lagrange multipliers and Tikhonov regularization; see Ref. 13.

Properties, advantages, and limitations of selected inversion techniques are compared in Refs. 21, 23, 24, and 25. In this respect, two important facts should be emphasized:

1. In modern plasma tomography, different inversion techniques can provide robust and similar solutions that fit data well. Major improvements of the plasma tomography performance can be achieved only through amendments of the contribution matrix (in particular, by improving coverage of the image by the line-integrated measurements, e.g., more regular coverage or increasing the number of cameras, and by their high-precision positioning) and by increased accuracy of data measurements.

2. There are no universal guidelines for the choice of any particular inversion technique. Indeed, different techniques may suit different purposes, as will be exemplified in Sec. III.

Because of the nature of ill-posed problems, it is paramount to assess the performance of the applied inversion technique and to validate the reliability of the reconstructed image (see also Ref. 1, Sec. IV.H). To this end the following procedures are used:

1. *Test runs using phantom images:* In the test runs, the tomography algorithm is applied to line-integrated data calculated from a model (phantom) image; see Ref. 23. The procedure has a clear advantage of direct comparison of the phantom and reconstructed image, with possible quantification of the misfit. However, it is rather challenging to obtain model data that would reflect in sufficient detail the experimental data behavior.

2. *Backfit of the reconstructed image, i.e., comparison of the reconstructed $\sum_j T_{ij} g_j$ with the measured line integrals f_i :* This simple and universal procedure validates the inversion and provides a tool for quantifying the reliability of individual channels. Moreover, the “goodness-of-fit” parameter χ^2 is often applied to optimize iteratively the regularization parameter (corresponding to the strength of smoothness) if data are sparse²¹:

$$\chi^2 = \frac{1}{N} \sum_{i=1}^N \frac{\left(f_i - \sum_j T_{ij} g_j\right)^2}{\sigma_i^2} \rightarrow 1. \quad (3)$$

Condition (3) requires that the backfit residuals are on average of the same amplitude as the expected errors σ_i ; that is, $\chi^2 < 1$ indicates overfitting, and $\chi^2 > 1$ indicates oversmoothing.

3. *Error transmission studies via Monte Carlo simulation:* Since the impact of statistical errors (data noise) and systematic errors (e.g., in the contribution matrix) on the resulting image cannot be universally predicted because of the ill-posed nature of the problem, it is recommended to quantify them statistically. For example, a simple Monte Carlo simulation of the error transmission can be implemented; see Ref. 16: The tomography inversion is run repetitively on fixed projection data (either synthetic or real) with variable additive noise, and resulting fluctuations in the reconstructed image are analyzed as a function of the noise amplitude and distribution. Alternatively, the error transmission can be quantified via Bayesian analysis.²⁶

The error transmission studies are rather demanding in terms of computational time, which gives an important advantage to inversion techniques with a high execution speed. Similar preference appears in the case of massive processing of large databases—see Ref. 27—and as a matter of course in the real-time application discussed in Sec. III. However, in contrast to the real-time tomography inversion, in the postprocessing applications the inversion techniques can benefit from normal access to data from other diagnostic systems.

Last, but not least, high temporal resolution of the line-integrated measurements presents another distinctive attribute of tomography of fusion plasmas, which is unmatched by medical or industrial systems. Although good knowledge of data evolution cannot compensate for missing information in the spatial coordinates—except for in very special cases; see Ref. 1, Sec. IV.I.3—it has a clear potential to improve data statistics. Only a few papers have recognized and exploited this fact so far, including Refs. 28 and 29 by the selection criterion for the expansion coefficients in the Cormack method, Refs. 21 and 25 by application of singular value decomposition (SVD) to evolution of reconstructed emissivity, and Ref. 27 by implementation of the time coordinate in Eq. (3) so that time-averaged regularization coefficients are derived.

III. SXR TOMOGRAPHY IN THE PROSPECT OF REAL-TIME CONTROL

As mentioned before, different plasma tomography techniques may suit different purposes, and in the case of the real-time applications for fusion plasmas, the execution speed becomes the foremost advantage. In this respect, some of the above-mentioned techniques (e.g., standard implementations of the Lagrange multipliers,¹³

maximum likelihood,³⁰ or the maximum entropy¹⁷) are severely handicapped as they are based on time-demanding iterative optimization algorithms. The implementation of a priori information and constraints in the inversion technique presents another important criterion; in particular, any call for data from other diagnostic systems impedes the real-time applications.

Direct semianalytical inversion techniques are very quick in principle, including the Cormack technique,¹⁴ the Fourier-Bessel technique,¹⁵ SVD or QR decompositions,³¹ and semianalytical solution of a generalized eigenproblem.²⁰ The Cormack and Fourier-Bessel techniques are particularly suitable for plasmas constrained by axial symmetries (circular plasmas). Very fast numerical algorithms also exist for sparse-matrix computations with rotational invariance in the viewing system³²; however, this is not relevant for typical plasma tomography diagnostic systems. For similar reasons, there are only limited possibilities for computational parallelization.

Techniques based on Tikhonov regularization^b—see Refs. 1, 21, 23, and 25—are worth attention for shaped plasmas with more general constraints. In its general meaning, Tikhonov regularization denotes any technique that introduces the inversion matrix M_{ji} , which solves Eq. (2) as follows:

$$g_j = \sum_i M_{ji} f_i ,$$

where

$$M_{ji} = \sum_k \left(\sum_l T_{kl}^T T_{lj} + \lambda \sum_m B_{km}^T w_m B_{mj} \right)^{-1} T_{kl}^T . \quad (4)$$

A priori information and constraints are implemented in the weight vector w_m and, of course, in the contribution matrix T_{ij} and the square matrix B_{km} that acts as the objective functional (smoothness operator). Figure 4 is a graphical representation of one row of the contribution matrix T_{ij} representing one SXR channel at JET and the corresponding column of the inversion matrix M_{ji} for two different objective functionals. Notice that as long as the regularization factor λ and the objective functional can be considered constant in time, the inversion matrix M_{ji} needs to be computed only once, making the inversion very quick.

In Fig. 4c, preferential smoothing along magnetic flux surfaces is introduced. Recent progress in plasma tomography with sparse data relies to a substantial degree on implementation of this a priori information^{13,33} based on reconstruction of magnetic data. Although detailed experimental studies unveiled limits in the relation between magnetic flux surfaces and the SXR emissivity,^{34,35} the benefit of the preferential smoothing can be clearly demonstrated; see Fig. 5, which shows the SXR

^bReferred to as Phillips-Tikhonov regularization in Ref. 1 and linear regularization in Refs. 21 and 25.

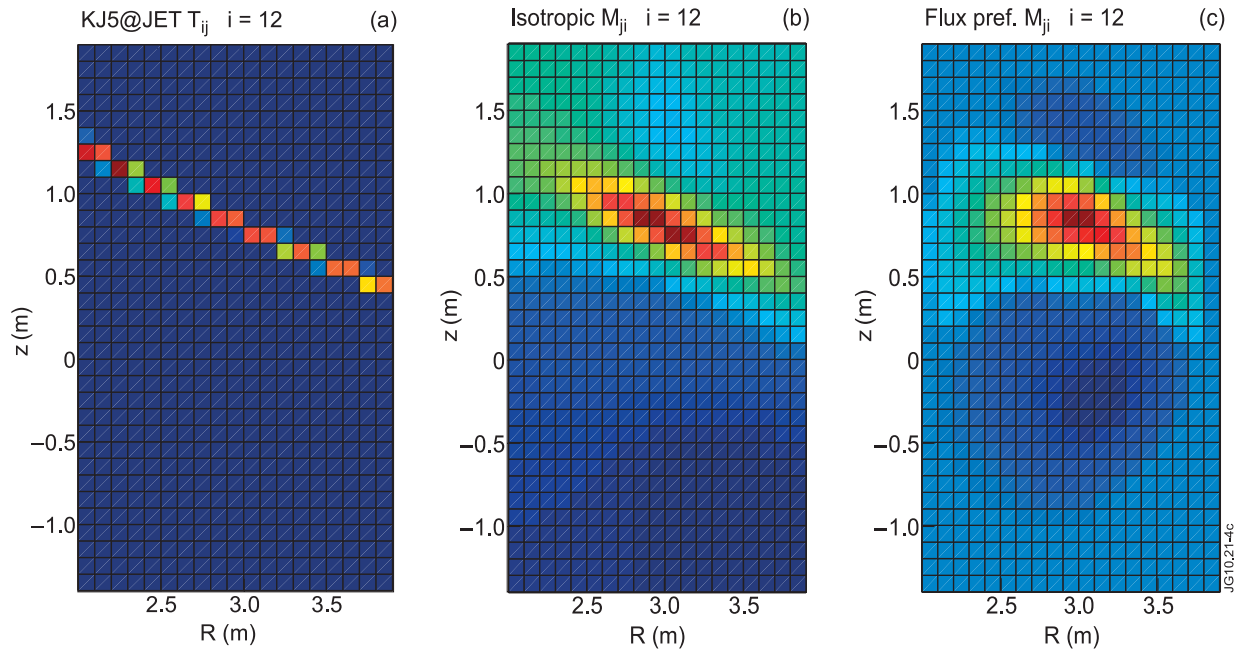


Fig. 4. Visual interpretation of the contribution and inversion matrices T_{ij} and M_{ji} . (a) The 12th row of T_{ij} corresponding to chord 12 of the present SXR tomography at JET in the regular mesh of pixels as in Fig. 3. (b) The 12th column of M_{ji} for isotropic smoothing. (c) The same column of M_{ji} for preferential smoothing along magnetic flux surfaces. Notice that (b) and (c) depend to some degree on regularization factors and, therefore, on the measured SXR data. A simple peaked emissivity distribution was applied in this example.

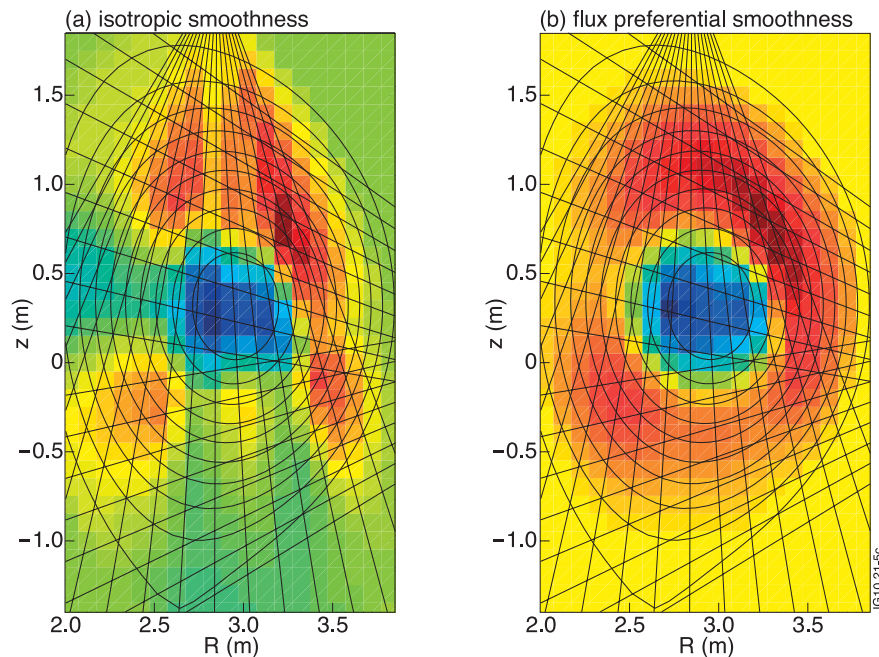


Fig. 5. Role of the objective functional in the example of the reconstructed SXR emissivity change at JET shortly after a major sawtooth crash in JET discharge #65942 at 18.3 s. (a) With isotropic smoothing, leading to an artifact image in the upper part. (b) With preferential smoothing along magnetic flux surfaces, clearly enforcing the expected poloidal symmetry. The emissivity change is quantified by the second moment of the SVD “topos” of the temporal evolution of the SXR emissivity inversion; see Ref. 21.

emissivity change just after a major sawtooth crash at JET. In Fig. 5a, due to sparse data, the inversion optimized to isotropic smoothness makes little physical sense (note the up-down asymmetry and strong correlation with the diagnostic geometry; compare with Fig. 3). In Fig. 5b, the inversion optimized to preferential smoothness along flux surfaces results in a smoother, more symmetric image. Implementation of a consecutive magnetic and SXR inversion is at present not achievable in real time; however, it will be acceptable to use predicted geometry of magnetic flux surfaces based on the plasma operation scenario (waveforms) due to robustness of the Tikhonov regularization with respect to uncertainties in additional information; see Refs. 16 and 27. Note in this respect that in Eq. (4) all additional information is implemented in the smoothness control only, while the geometric setup is fixed by the contribution matrix T_{ij} independently of the geometry of the flux surfaces.

A more serious challenge for real-time implementation of the Tikhonov regularization comes from the fact that in the present algorithms the regularization factor λ and nonlinear objective functionals (e.g., the minimum Fisher information²¹) are optimized in a few iterative loops that, however rapid, may prove inadequate for real-time applications. The direct semianalytical²⁰ or QR decomposition³¹ techniques are closely related to the iterative Tikhonov regularization and may offer a solution; however, their potential and adequacy for the real-time applications is yet to be demonstrated.

Novel inversion techniques for sparse data based on neural networks²² are at present under development for real-time tomography of shaped plasmas.^{36,37} Neural networks require a well-prepared and sufficiently general training on phantom images, which is quite demanding in execution time; however, the subsequent inversions are very rapid. At JET, the neural networks were successfully trained and applied for tomography of neutron emission³⁶ and for analyses of bolometric data³⁸ (with the training set derived from the tomography inversions), both with a prospect of real-time applications. A project on neural network application for SXR real-time tomography is pursued for the W7-X stellarator including detailed realistic training.³⁷ The work demonstrates that neural networks are very rapid and robust for image parameters close to the training set; however, the technique tends to create major artifacts when extrapolation rather than interpolation from the known phantom images is required.

The real-time capabilities of inversion techniques go hand in hand with hardware developments, and the difficulties on the engineering side of the real-time systems are not to be underestimated. Pioneering work was done at JET using transputers.³⁹ In Ref. 40, three hardware options are discussed, with the conclusion that a CPCI-Pentium system is adequate for the required 10-ms operational deadline. At present, there is little doubt that hardware can be sufficiently powerful to implement a rapid inversion software with acceptable spatial and temporal

properties; however, design of the corresponding system is still far from routine. A rather rare example of working real-time hardware for a SXR tomography system is presented in Ref. 41, with field-programmable gate array (FPGA) data processing and an ATX motherboard running real-time application interface (RTAI) for Linux.

IV. CONCLUDING REMARKS

In the current fusion research, tomography offers a direct, data-driven alternative to forward-fitted models in studies of plasma emissivity. Specialized inversion techniques must be applied in plasma tomography because of sparse projection data, and for the same reason, the spatial resolution of the tomography inversion remains rather low. This weakness can be partly relieved by proper implementation of a priori information and constraints. Tests on phantom distributions—among other procedures—help to validate objective information and detect possible artifacts in the resulting image linked to the ill-posedness of the task.

Soft-X-ray diagnostics represents a very attractive candidate for tomography applications, with relatively inexpensive detectors, high temporal resolution, and high relevance of the data to the physics of plasma core. Because of progress in both software and hardware development, real-time SXR tomography based on dedicated rapid inversion techniques is feasible, with the potential to support the control of plasma position, plasma stability, and impurity content.

It is quite difficult (if not impossible) to identify a unique inversion technique as the best solution for real-time SXR tomography of fusion plasmas. Discussion in Sec. III indicated that the Tikhonov regularization and neural networks represent competitive rapid inversion techniques for a wide range of possible emissivities of shaped plasmas. Interestingly, the limitations of the two techniques are complementary: (a) The Tikhonov regularization requires optimization of a few coefficients but proves robust in tomography inversion of any consistent data, while (b) the neural network, once it is trained, needs no optimization loops but fails to reconstruct reliably data differing from the training set. Therefore, a possible merger of the two techniques, with neural network trained to predict optimal regularization coefficients for a direct setup of the inversion matrix according to the Tikhonov regularization, can be proposed. The feasibility and performance of this novel technique need to be demonstrated and benchmarked against other existing rapid methods including the above-mentioned semi-analytical²⁰ and QR decomposition³¹ techniques.

ACKNOWLEDGMENTS

The authors wish to thank Ch. Ingesson for his helpful comments. This work, supported by grants GA CR 205/10/

2055, GA CR 202/09/1467, and MSMT LA08048, and by the European Communities under the contract of Association between EURATOM and IPP.CR, Belgian state, and ENEA, was carried out within the framework of the European Fusion Development Agreement. The views and opinions expressed herein do not necessarily reflect those of the European Commission.

REFERENCES

1. L. C. INGESSON, B. ALPER, B. J. PETERSON, and J.-C. VALLET, "Tomography Diagnostics: Bolometry and Soft X-Ray Detection," *Fusion Sci. Technol.*, **53**, 528 (2008).
2. M. B. McGARRY et al., "Multicolor SXR Tomography on MST," presented at American Physical Society 50th Annual Meeting of Division of Plasma Physics, Dallas, Texas, November 17–21, 2008; <http://plasma.physics.wisc.edu/uploadedfiles/talk/apsdpp08McGarry532.pdf> (current as of Mar. 15, 2010).
3. L. GABELLIERI et al., "A Simplified Automatic Method to Infer Information About Impurity Content and Spatial Distribution in Tokamak Plasmas," *Europhysical Conference Abstracts: 36th Conf. Plasma Physics*, Sofia, Bulgaria, June 29–July 3, 2009, Vol. 33E, p. P4.201, European Physical Society (2009).
4. A. INCE-CUSHMAN et al., "Spatially Resolved High Resolution X-Ray Spectroscopy for Magnetically Confined Fusion Plasmas," *Rev. Sci. Instrum.*, **79**, 10E302 (2008).
5. S. YAMAGUCHI, H. IGAMI, H. TANAKA, and T. MAEKAWA, "Three-Dimensional Observation of an Helical Hot Structure During a Sawtooth Crash in the WT-3 Tokamak," *Phys. Rev. Lett.*, **93**, 045005 (2004).
6. J. P. QIAN et al., "Equilibrium Reconstruction of Plasma Profiles Based on Soft X-Ray Imaging in DIII-D," *Nucl. Fusion*, **49**, 025003 (2009).
7. A. MURARI et al., "'Burning Plasma' Diagnostics for the Physics of JET and ITER," *Plasma Phys. Control. Fusion*, **47**, B249 (2005).
8. Yu. V. GOTT and M. M. STEPANENKO, "Vacuum Photodiode Detectors for Soft X-Ray ITER Plasma Tomography," *Rev. Sci. Instrum.*, **76**, 073506 (2005).
9. D. PACELLA and D. MAZON, "Soft X-Ray Diagnostics and Treatments for Future Real Time Applications," *AIP Conf. Proc.*, **988**, 405 (2008).
10. A. MURARI et al., "Development of Real-Time Diagnostics and Feedback Algorithms for JET in View of the Next Step," *Plasma Phys. Control. Fusion*, **47**, 3, 395 (2005).
11. G. T. HERMAN, *Fundamentals of Computerized Tomography*, Springer-Verlag London Limited (2009).
12. V. WEINZETTL et al., "Design of Multi-Range Tomographic System for Transport Studies in Tokamak Plasmas," *Nucl. Instrum. Methods Phys. Rev. A* (2010) (to be published); doi:10.1016/j.nima.2010.04.010.
13. L. C. INGESSON et al., "Soft X Ray Tomography During ELMs and Impurity Injection in JET," *Nucl. Fusion*, **38**, 1675 (1998).
14. A. M. CORMACK, "Representation of a Function by Its Line Integrals, with Some Radiological Applications. II," *J. Appl. Phys.*, **35**, 2908 (1964).
15. L. WANG and R. S. GRANETZ, "An Analytical Expression for the Radon Transform of Bessel Basis Functions in Tomography," *Rev. Sci. Instrum.*, **62**, 1115 (1991).
16. G. BONHEURE et al., "A Novel Method for Trace Tritium Transport Studies," *Nucl. Fusion*, **49**, 8, 085025 (2009).
17. K. ERTL et al., "Maximum Entropy Based Reconstruction of Soft X Ray Emissivity Profiles in W7-AS," *Nucl. Fusion*, **36**, 1477 (1996).
18. J. KIM and W. CHOE, "Fast Singular Value Decomposition Combined Maximum Entropy Method for Plasma Tomography," *Rev. Sci. Instrum.*, **77**, 023506 (2006).
19. P. C. HANSEN, "Numerical Tools for Analysis and Solution of Fredholm Integral Equations of the First Kind," *Inverse Problems*, **8**, 849 (1992).
20. G. C. FEHMERS, L. P. J. KAMP, and F. W. SLUIJTER, "An Algorithm for Quadratic Optimization with One Quadratic Constraint and Bounds on the Variables," *Inverse Problems*, **14**, 893 (1998).
21. M. ANTON et al., "X-Ray Tomography on the TCV Tokamak," *Plasma Phys. Control. Fusion*, **38**, 1849 (1996).
22. G. DEMETER, "Tomography Using Neural Networks," *Rev. Sci. Instrum.*, **68**, 1438 (1997).
23. T. CRACIUNESCU et al., "A Comparison of Four Reconstruction Methods for JET Neutron and Gamma Tomography," *Nucl. Inst. Methods Phys. Res. A*, **605**, 3, 374 (2009).
24. J. KIM, S. H. LEE, and W. CHOE, "Comparison of the Three Tokamak Plasma Tomography Methods for High Spatial Resolution and Fast Calculation," *Rev. Sci. Instrum.*, **77**, 10F513 (2006).
25. A. K. CHATTOPADHYAY, A. ANAND, and C. V. S. RAO, "Tomography for SST-1 Tokamak with Pixel Method," *Rev. Sci. Instrum.*, **76**, 063502 (2005).
26. S. KÁLVIN and L. C. INGESSON, "Performance Analysis of ITER Tomographic Systems," *AIP Conf. Proc.*, **988**, 485 (2008).
27. J. MLYNAR et al., "Investigation of the Consistency of Magnetic and Soft X-Ray Plasma Position Measurements on TCV by Means of a Rapid Tomographic Inversion Algorithm," *Plasma Phys. Control. Fusion*, **45**, 2, 169 (2003).
28. Yu. N. DNESTROVSKIY, E. S. LYADINA, and P. V. SAVRUKHIN, "The Space-Time Tomographic Problem of Plasma Diagnostics," *Sov. J. Plasma Phys.*, **18**, 107 (1992).

29. E. S. LYADINA et al., "A Space-Time Tomography Algorithm for the Five-Camera Soft X-Ray Diagnostic at RTP," *Europhysics Conference Abstracts: 20th Conf. Controlled Fusion and Plasma Physics*, Lisbon, Portugal, July 26–30, 1993, Vol. 17C, Part III, p. 1151, European Physical Society (1993).
30. T. CRACIUNESCU et al., "The Maximum Likelihood Reconstruction Method for JET Neutron Tomography," *Nucl. Instrum. Methods Phys. Res. A*, **595**, 623 (2008).
31. N. TERASAKI et al., "Linear Algebraic Algorithms for High Speed and Stable Reconstruction of Plasma Image," *Fusion Eng. Des.*, **34–35**, 801 (1997).
32. J. R. BAKER, T. F. BUDINGER, and R. H. HUESMAN, "Generalized Approach to Inverse Problems in Tomography: Image Reconstruction for Spatially Variant Systems Using Natural Pixels," *Crit. Rev. Biomed. Eng.*, **20**, 47 (1992).
33. G. FUCHS, Y. MIURA, and M. MORI, "Soft X-Ray Tomography on Tokamaks Using Flux Coordinates," *Plasma Phys. Control. Fusion*, **36**, 307 (1994).
34. R. S. GRANETZ and M. C. BORRÁS, "Is X-Ray Emissivity Constant on Magnetic Flux Surfaces?" *Fusion Eng. Des.*, **34–35**, 153 (1997).
35. C. P. TANZI, H. J. DE BLANK, and A. J. H. DONNÉ, "A New Approach to Internal Disruption Analysis with the Five-Camera Soft-X-Ray Diagnostic on RTP," *Rev. Sci. Instrum.*, **66**, 537 (1995).
36. E. RONCHI et al., "Neural Networks Based Neutron Emissivity Tomography at JET with Real-Time Capabilities," *Nucl. Instrum. Methods Phys. Res. A*, **613**, 295 (2010).
37. H. THOMSEN et al., "Application of Neural Networks for Fast Tomographic Inversion on Wendelstein 7-X," *Europhysics Conference Abstracts: 35th Conf. Plasma Physics*, Crete, Greece, June 9–13, 2008, Vol. 32D, p. P-1.065, European Physical Society (2008).
38. O. BARANA et al., "Neural Networks for Real Time Determination of Radiated Power in JET," *Rev. Sci. Instrum.*, **73**, 2038 (2002).
39. E. VAN DER GOOT, A. W. EDWARDS, and J. HOLM, "Real Time Application of Transputers for Soft X-Ray Tomography in Nuclear Fusion Research," *Proc. 1st Int. Conf. Applications of Transputers*, Liverpool, United Kingdom, August 23–25, 1989, p. 306, IOS (1990).
40. J. MLYNAR, B. P. DUVAL, J. HORACEK, and J. B. LISTER, "Present and Perspective Roles of Soft X-Ray Tomography in Tokamak Plasma Position Measurements," *Fusion Eng. Des.*, **66–68**, 905 (2003).
41. P. J. CARVALHO et al., "Real-Time Plasma Control Based on the ISTTOK Tomography Diagnostic," *Rev. Sci. Instrum.*, **79**, 10, 10F329 (2008).